Pergamon

Planet. Space Sci., Vol. 44, No. 6, pp. 529–539, 1996

0032-0633/96 $15.00+0.00

PII: S0032-0633(96)00015-3

Radio line observations of comet 109P/Swift–Tuttle at IRAM

D. Despois,[1] N. Biver,[2] D. Bockelée-Morvan,[2] P. Colom,[2] J. Crovisier[2] and G. Paubert[3]

[1]Observatoire de Bordeaux, B.P. 89, F-33270 Floirac, France
[2]Observatoire de Paris, Section de Meudon, F-92195 Meudon, France
[3]IRAM, Avenida Divina Pastora 7, E-18012 Granada, Spain

Received 1 October 1993; revised 10 January 1996; accepted 10 January 1996

Abstract. Observations are presented of comet 109P/Swift–Tuttle (1992t and 1992 XXVIII in the old style designations) obtained at the IRAM 30 m millimetre radio telescope both before (Nov. 1992) and after perihelion (Jan. 1993), when r_h was ~ 1 AU and Δ between 1 and 2 AU. The molecules HCN, H_2S, H_2CO and CH_3OH were detected, with good signal-to-noise ratios (up to 30). The line profiles are strongly asymmetric with a cusp at negative velocities; this leads to an important shift (-0.45 km s^{-1}) of the mean gas velocity with respect to the nucleus. This profile is most probably linked to the jets seen at visual wavelengths. From methanol rotation diagrams, average rotational temperatures of 70 K for November 21 and 45 K for January are estimated. An isotropic distribution of the molecules is assumed, and $Q(H_2O) \sim 4.0$ and 3.5×10^{29} molec. s^{-1} for November 21 and January, respectively. Relative production rates $Q/Q(H_2O)$ of 0.1, 0.4, 0.5 and 4–7% on November 21, 1992 for HCN, H_2S, H_2CO and CH_3OH, respectively, and 0.05, 0.2 and 2% on January 6–7, 1993, for HCN, H_2CO and CH_3OH, respectively, are derived. The effect of coma anisotropy on the derivation of these rates is briefly discussed. The decrease of non-water parent molecules from November to January, to be confirmed, raises questions about the nucleus homogeneity or sublimation process. Copyright © 1996 Published by Elsevier Science Ltd

1. Introduction

109P/Swift–Tuttle is a periodic comet in a high-inclination orbit. With a period of about 130 years it belongs to the short-period, Halley-type comet class. This intrinsically bright object was discovered at its preceding passage under very favourable conditions (minimal distance to the Earth $\Delta_{min} = 0.3$ AU), and will again pass at a small—but fortunately non-zero—distance from the Earth in 2126 ($\Delta_{min} \sim 0.15$ AU; Yau *et al.*, 1993; Marsden *et al.*, 1993). The earliest match of a P/Swift–Tuttle passage with an historical record of a comet-like phenomenon dates from 69 B.C., but it has probably haunted the inner Solar System for many years before. Its Earth-crossing orbit makes it deliver regularly material to the Earth through a well-known meteor stream, the Perseids (seen in August), as was shown by Schiaparelli (1867).

Well-defined jets in the coma are the most striking aspect of this comet (Sekanina, 1984; Jorda *et al.*, 1994). They suggest the presence of several active zones on the nucleus. The shape and time evolution of these jets is a clue to the determination of the nucleus spin period, which is about 2.8 days. An important result of the radio observations of P/Swift–Tuttle is the finding of a very asymmetric line profile for all species, which is most probably the manifestation in velocity space of the spatial anisotropy of the coma.

Radio observations of comet P/Swift–Tuttle are at one and the same time a successful new step in the investigation of parent molecule abundances in cometary comae through the radio technique and the study of a very interesting individual comet. Since the first unambiguous detection of HCN in comet Halley (Bockelée-Morvan *et al.*, 1987; Schloerb *et al.*, 1987), H_2CO, H_2S and CH_3OH have been successively observed in cometary comae, due to the increase of telescope sensitivity and frequency coverage (see Crovisier (1992b) for a review).

Despite a not very favourable position of the comet with respect to the Earth, our radio observations conducted with the 30 m radio telescope of the Institut de Radio Astronomie Millimétrique (IRAM) were very successful, all four species mentioned above being detected with good signal-to-noise ratios (up to 30). Several other groups observed P/Swift–Tuttle at millimetre wavelengths, with the following radio telescopes: JCMT (Bockelée-Morvan *et al.*, 1994c); CSO (Schloerb *et al.*,

Correspondence to: D. Bockelée-Morvan

1993; Womack and McKeown, 1993); NRAO 12 m (Wootten *et al.*, 1994; Womack and McKeown, 1993).

We present in the following a detailed report of these observations (Section 2). We then derive column densities averaged over the beam for all four species using the excitation models developed in our preceding studies (Section 3). Production rates (absolute and relative to H_2O) are presented in Section 4, assuming an isotropic distribution of the molecules; this is only a crude approximation for comet P/Swift–Tuttle, and a more realistic model of the coma will be developed in a future paper. Various points, including coma anisotropy and line shapes are discussed in Section 5.

2. Observations

The observations took place at the 30 m millimetre radio telescope of the Institut de Radio Astronomie Millimétrique (IRAM) on Pico Veleta (Spain). There were three different periods: two of them (Nov. 11–14 and Nov. 21, 1992) preceded and one (Jan. 6–7, 1993) followed the perihelion, which took place on December 12. Although the comet was never very close to the Earth, the molecular lines we searched for were always detected, often with rather high signal-to-noise ratio, due to the good sensitivity of the instrument and to the intrinsic brightness of the comet.

The distance of the comet to the Sun r_h remained nearly constant (between 1.0 and 1.1 AU) during our observations, whereas its configuration with respect to the Earth changed markedly, the distance Δ increasing from 1.2 to 2.0 AU, and the Earth–comet–Sun angle (phase angle) decreasing from about 50° to 15°.

Due to the long orbital period, precise astrometric positions from previous passages are scarce, and the present return was in fact first predicted to take place in 1981, although 1992 was a possible second choice (Marsden, 1973). Even after its rediscovery by Kiuchi (1992) at the end of September 1992, it took some time to get a really accurate set of orbital elements. Three successive sets of elements of improving accuracy were used for our radio observations. The inaccuracy of the first ones results in offsets of up to 15″ for some of our early observations which were in principle aimed at the nucleus position. Table 1 gives these offsets using an actual nucleus position based on the precise orbital elements given by Marsden *et al.* (1993).

Pointing and focus were regularly checked and corrected on nearby galactic sources or planets. Special care was taken for the low-elevation observations of January 1993, where Mercury, close in declination to the comet but with an hour angle larger by 2 h, was monitored in advance. The resulting telescope pointing accuracy was on the order of 2″ r.m.s. for the receiver used as a reference. All receivers were aligned within a few arc seconds, the largest offset being 4″ between the 3 mm receiver (used for pointing) and the 1.3 mm receiver on Jan. 6, 1993 (accounting for this offset would change the production rate by less than 20%).

In each of the three periods we observed (i) the HCN (1–0) line at 88.6 GHz, (ii) the H_2CO 3_{12}–2_{11} line at 225 GHz, and (iii) the CH_3OH group of lines around 145 GHz; in addition observed in November where (iv) a second group of methanol lines around 165 GHz, and (v) the H_2S 1_{10}–1_{01} line at 168 GHz. In January, due to technical reasons, only two receivers instead of three could be used simultaneously. The SIS mixers were tuned single side-band (SSB) with an image band rejection of 7 dB or better, except for the 165 GHz observations, where it was only 5 dB.

To analyse the signals we used various combinations of the following backends: (i) two banks of 512×1 MHz filters; (ii) a bank of 256×100 kHz filters; (iii) two different units of an autocorrelator, in the modes 39 and 78 kHz channel separation (with a total of 1024 channels in each case); (iv) a 1024×800 kHz (channel separation) AOS device. Table 2 details the frequency and backend setting for each day.

The weather was in general fine, except on Nov. 11 where clouds prevented good observations in the last part of the day. Two days were very good, Nov. 21 and Jan. 7, with a water content below 2–3 mm. On Nov. 21, the zenith opacity was below 0.2 at all frequencies, and the SSB system temperatures towards the comet and outside the atmosphere, T_{sys}*, were around 350, 470, 700 and 1050 K at 89, 145, 165 and 225 GHz, respectively. The comet culminated above 70° in November, and at 29° in January. Table 2 gives the r.m.s. noise per channel which was achieved on each day at the various frequencies.

The data were calibrated using a standard hot–cold load procedure (e.g. Guilloteau, 1987) to give antenna temperatures outside the atmosphere, and a linear baseline was subtracted from all spectra. The line calibration was checked 2–3 times per day on the galactic sources W51 E1/E2 or W51 D (cf. Mauersberger *et al.*, 1989).

Table 1. Orbital elements actually used for the observations and comet position

Date	r_h [AU]	Δ [AU]	Phase	Orbital elements	Offset[a] α ["]	δ ["]
921111.6	1.092	1.173	51.6	MPC 21081	−4.9	13.7
921112.6	1.084	1.177	51.7	"	−4.8	13.9
921114.6	1.069	1.187	51.7	"	−4.5	14.3
921121.6	1.021	1.250	50.5	[b]	−0.3	−2.7
930106.5	1.051	1.961	14.9	MPC 21235	0.7	0.2
930107.5	1.058	1.974	14.3	"	0.7	0.3

[a][observed position]−[position from Marsden *et al.* (1993)].
[b]Marsden, private communication, 19 Nov. 1992.

Table 2. Log of the observations

Date (UT)	[a] [min]	Line		Frequency [MHz][b]	Backend[c]		r.m.s. [mK]
921111.544–.837	256	HCN	(1–0)	88,631.847	FB	1 MHz	6
					A/C	39 kHz	28
921111.544–.837	256	CH_3OH	145	145,103.234	FB	1 MHz	9
					A/C	78 kHz	30
921111.544–.837	256	H_2CO	3_{12}–2_{11}	225,697.772	AOS		30
					FB	100 kHz	91
921112.543–.838	265	HCN	(1–0)	88,631.847	FB	1 MHz	6
					A/C	39 kHz	26
921112.543–.838	265	H_2S	1_{10}–1_{01}	168,762.782	FB	1 MHz	21
					A/C	78 kHz	67
921112.543–.838	255	H_2CO	3_{12}–2_{11}	225,697.772	AOS		21
					FB	100 kHz	68
921114.503–.706	183	HCN	(1–0)	88,631.847	FB	1 MHz	5
					A/C	39 kHz	24
921114.503–.706	196	CH_3OH	165	165,125.000	FB	1 MHz	14
					A/C	78 kHz	41
921114.503–.706	196	H_2CO	3_{12}–2_{11}	225,697.772	AOS		17
					FB	100 kHz	54
921121.426–.813	300	HCN	(1–0)	88,631.847	FB	1 MHz	5
					A/C	39 kHz	20
921121.426–.506	67	CH_3OH	145	145,103.234	FB	1 MHz	11
					A/C	78 kHz	35
921121.525–.645	100	CH_3OH	165	165,210.000	FB	1 MHz	16
					A/C	78 kHz	57
921121.664–.813	133	H_2S	1_{10}–1_{01}	168,762.782	FB	1 MHz	13
					A/C	78 kHz	41
921121.426–.813	300	H_2CO	3_{12}–2_{11}	225,697.772	AOS		14
					FB	100 kHz	35
930106.471–.701	180	HCN	(1–0)	88,631.847	FB	1 MHz	6
					A/C	39 kHz	26
930106.471–.701	180	H_2CO	3_{12}–2_{11}	225,697.722	FB	1 MHz	23
					A/C	78 kHz	83
					FB	100 kHz	68
930107.409–.700	198	HCN	(1–0)	88,631.847	FB	1 MHz	5
					A/C	39 kHz	22
					FB	100 kHz	12
930107.510–.700	156	CH_3OH	145	145,103.234	FB	1 MHz	6
					A/C	78 kHz	21

[a] Integration time.
[b] Central frequency of the observation (main side-band).
[c] Backend: filter bank (FB), autocorrelator (A/C) or acousto-optic spectrometer (AOS) with the channel separation (which may differ from the effective spectral resolution); the r.m.s. noise is given for a channel.

The line area on the calibrator remained constant within $\pm 10\%$ at 3 and 2 mm, and within $\pm 20\%$ at 1.3 mm. The antenna temperature was converted to main beam brightness temperature using the efficiencies in Table 3; comparison with other telescopes is then possible using the beam width given in the same table together with a model of the spatial distribution of the molecules.

Table 3. Telescope parameters: half-power beam width θ_B, aperture efficiency η_A, main beam efficiency η_B

ν [GHz]	θ_B ["]	η_A	η_B
88.6	27.0	0.9	0.64
145.0	16.0	0.88	0.56
165.0	14.5	0.88	0.53
168.0	14.5	0.88	0.53
225.0	12.0	0.9	0.46

3. Results and analysis

Figures 1 and 2 show the spectra obtained on Nov. 21 and Jan. 6–7. The line parameters (integrated area and velocity shift) for each transition of HCN, H_2S, H_2CO, CH_3OH and for each individual day are summarized in Tables 4 and 5.

To derive the molecular column density averaged over the beam, we use the same molecular parameters and excitation model as in our previous studies (Crovisier, 1987: HCN; Colom *et al.*, 1992; Bockelée-Morvan and Crovisier, 1992: H_2CO; Crovisier *et al.*, 1991: H_2S; Bock-

elée-Morvan *et al.*, 1994b: CH_3OH). These models follow the evolution of the populations of the relevant rotational and vibrational molecular levels from the collision-dominated inner coma to the fluorescence-dominated outer coma. They make use of approximate collision cross-sections with H_2O, together with assumptions on the kinetic temperature distribution through the coma, and standard solar spectral intensity data.

The case of CH_3OH is somewhat different, since we can take advantage of the numerous detected lines. We used the rotation diagram technique which allows the derivation of the rotational temperature and gives a direct access to the column density almost independently of any detailed model assumption on the excitation conditions, provided one is not too far from LTE conditions. These diagrams are shown in Fig. 3. The *A* and *E* type methanol have been treated as a unique species: their abundance ratio is not expected to differ much from one for the formation temperatures commonly assumed (Crovisier, 1992a); with only three lines available for the *A* species, such a tiny effect, if present, would be within the noise.

On Nov. 21 both the 145 and 165 GHz groups of methanol lines are well fitted with a temperature on the order of 70 K: the rotational temperatures retrieved from the rotation diagrams are 74 ± 22 and 67 ± 28 K for the 145 and 165 GHz lines, respectively. As detailed in Bockelée-

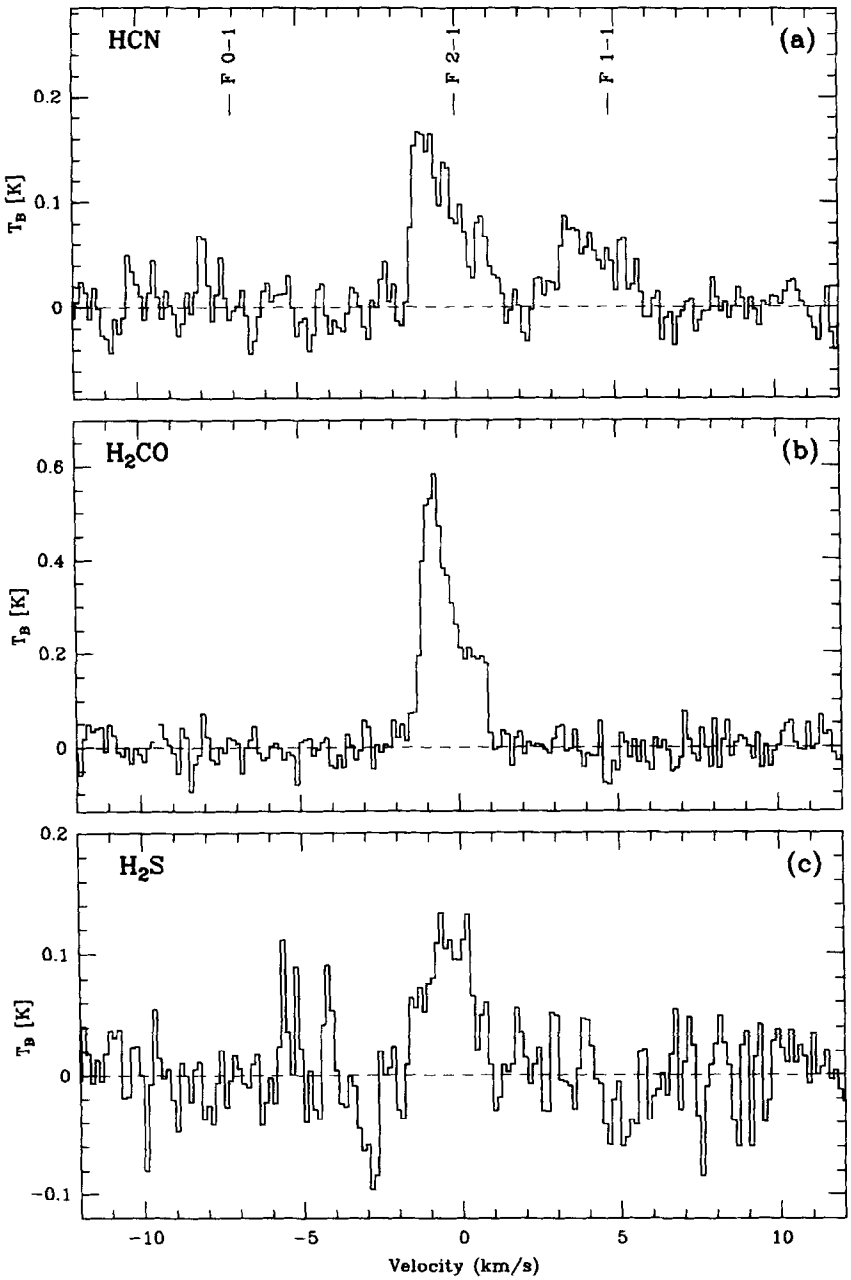

Fig. 1. Millimetre wave spectra of 109P/Swift–Tuttle on Nov. 21, 1992 at IRAM. (a) HCN (1–0) line at 88.6 GHz; (b) H_2CO 3_{12}–2_{11} line at 225 GHz; (c) H_2S 1_{10}–1_{01} line at 168 GHz; (d) CH_3OH lines around 145 GHz; (e) CH_3OH lines around 165 GHz. The spectral resolution is (a) 39 kHz; (b) 100 kHz; (c) 78 kHz; (d) 78 kHz; (e) 1 MHz. The velocity scale is with respect to the comet rest velocity. The upper scale on the methanol spectra gives the rest frequency in MHz. The line intensity is main beam brightness temperature T_B in K

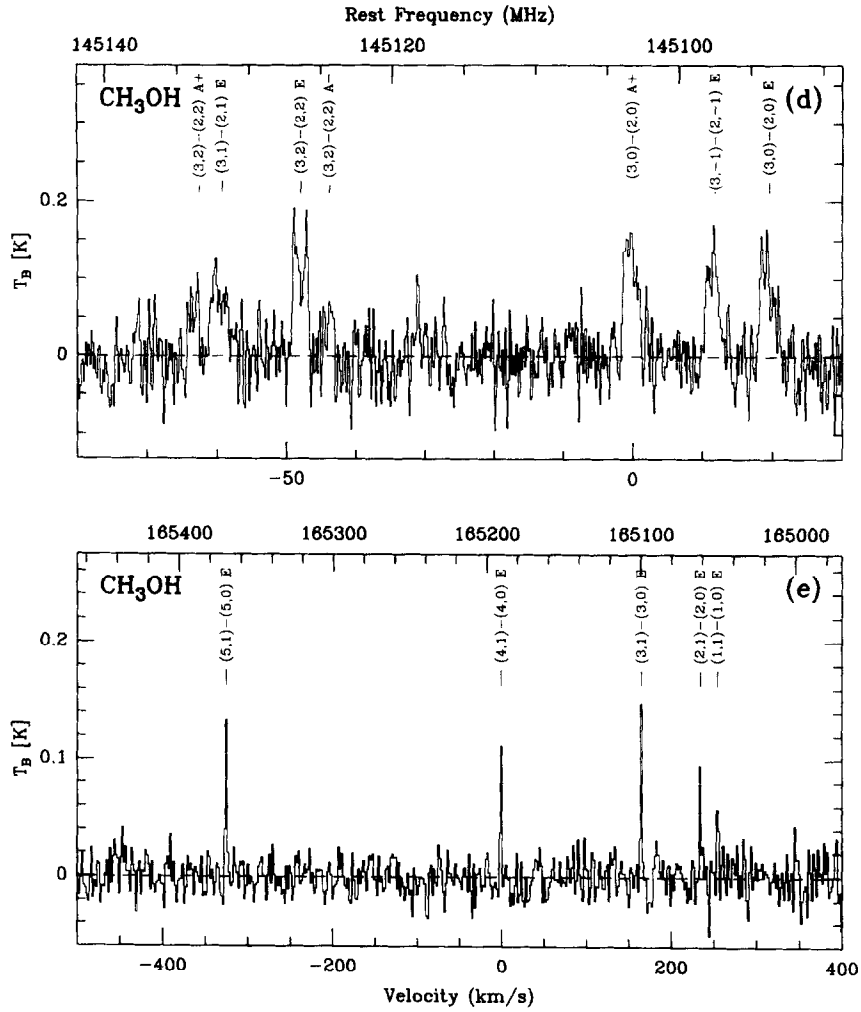

Fig. 1. (*Continued*).

Table 4. Line area $\int T_B dv$ and velocity shift δv for HCN, H_2CO and H_2S

Date	$\int T_B dv$ [K km s^{-1}]	δv^a [km s^{-1}]
(a) HCN (1–0) ν = 88.631847 GHz[b]		
Nov. 11	0.296±0.031	−0.45±0.07
Nov. 12	0.272±0.030	−0.38±0.06
Nov. 14	0.214±0.026	−0.48±0.13
Nov. 21	0.464±0.023	−0.41±0.04
Jan. 6	0.209±0.029	−0.60±0.20
Jan. 7	0.112±0.022	−0.50±0.20
(b) H_2CO $3_{1,2}$–$2_{1,1}$ ν = 225.697772 GHz		
Nov. 11	0.190±0.055	
Nov. 12	0.210±0.037	−0.45±0.12
Nov. 14	0.175±0.030	
Nov. 21	0.750±0.020	−0.42±0.02
Jan. 6	0.210±0.042	−0.77±0.23
(c) H_2S 1_{10}–1_{01} ν = 168.762782 GHz		
Nov. 21	0.210±0.025	−0.44±0.10

[a] First-order moment of the lines.
[b] The area is the sum of all three hyperfine components; the velocity shift has been computed from the main components $F(2\ 1)$ and $F(1\ 1)$.

Morvan *et al.* (1994b), this strongly suggests that observations were sampling molecules at thermal equilibrium. The column densities deduced from the 145 and 165 GHz lines differ by 50% (cf. Table 6); this difference is larger than expected from usual calibration uncertainties (±20%), and requires further investigation. From our 145 GHz January data, we obtain a lower temperature, 45±16 K, but the fit is of lesser quality and deviations from LTE populations may be present. A detailed modelling of the excitation conditions of methanol in comet P/Swift–Tuttle, as previously performed for comets Austin 1990 V and Levy 1990 XX (Bockelée-Morvan *et al.*, 1994b), will be needed to test whether this cold temperature is indeed indicative of cold thermal equilibrium or is characteristic of an out-of-equilibrium population distribution. It is predicted that, in the latter case, the column density is larger than that deduced from the rotation diagram analysis and given in Table 6; the underestimate may reach a factor of 2.

Although the kinetic temperature in the coma could in principle be given by thermodynamical calculations in the coma, such models have not yet enough constraints to give precise answers. We prefer to use instead, as the mean temperature in the range of the coma where the molecules

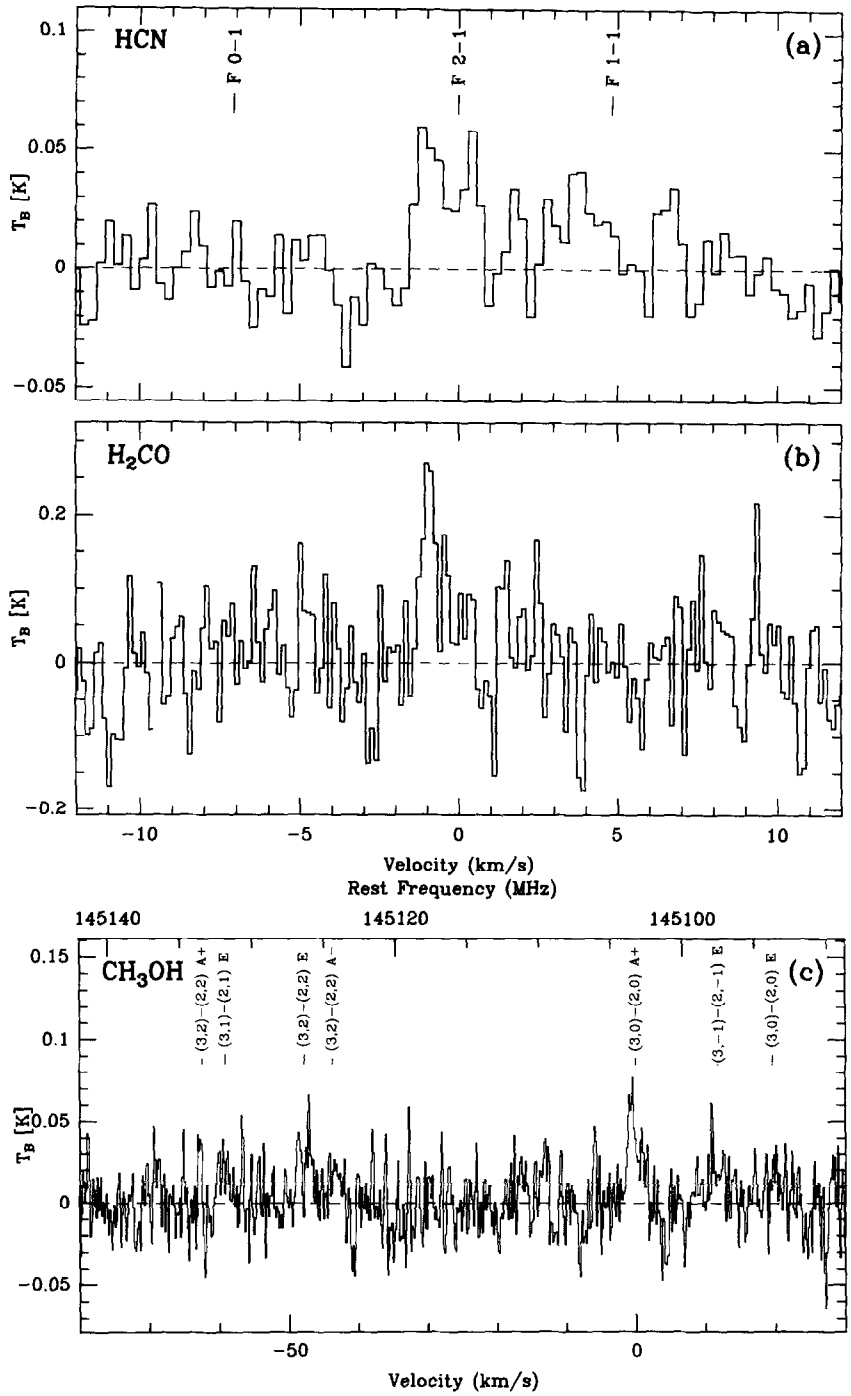

Fig. 2. Millimetre wave spectra of 109P/Swift–Tuttle in Jan. 1993 at IRAM. (a) HCN (1–0) line (average of Jan. 6 and 7); (b) H_2CO 3_{12}–2_{11} line at 225 GHz (Jan. 6); (c) CH_3OH lines at 145 GHz (Jan. 7). The spectral resolution is (a) 78 kHz; (b) 100 kHz; (c) 78 kHz. The velocity scale is with respect to the comet rest velocity. The upper scale on the methanol spectrum gives the rest frequency in MHz. The line intensity is main beam brightness temperature T_B in K

are present, the temperature that we deduced from the relative intensities of the CH_3OH lines. We adopt a value of 80 K for the Nov. 21 data, and a value of 40 K for the January data.

As in our previous studies, we have assumed a collisional cross-section of 10^{-14} cm^2. We found that, for the long-lived HCN molecule, the inferred column densities and production rates are strongly sensitive to the assumed collisional cross-section. Calculations with 10^{-13} cm^2 give values larger by a factor on the order of 2. We note that such a large cross-section is needed to reconcile the IRAM HCN observations with the JCMT ones (Bockelée-Morvan *et al.*, 1994c). Larger collision rates also help to bring closer together the relative molecular abundances derived for the November and the January periods (Biver *et al.*, in preparation).

Table 5. Methanol lines: line area $\int T_B dv$

Line	Frequency [GHz]	Date	$\int T_B dv$[a] [K km s^{-1}]
(3, 0)–(2, 0) *E*	145.09375	Nov. 11	<0.07
(3, −1) (2, −1) *E*	145.09747		0.102±0.021
(3, 0)–(2, 0) *A*+	145.10323		0.134±0.019
(3, 2) (2, 2) *A*+	145.12441		<0.062
(3, 2) (2, 2) *E*	145.12620		0.058±0.022[b]
(3, −2) (2, −2) *E*	145.12635		
(3, 1) (2, 1) *E*	145.13188		0.059±0.022
(3, 2) (2, 2) *A*−	145.13346		<0.063
(3, 0) (2, 0) *E*	145.09375	Nov. 21	0.293±0.029
(3, −1) (2, −1) *E*	145.09747		0.325±0.029
(3, 0) (2, 0) *A*+	145.10323		0.345±0.029
(3, 2) (2, 2) *A*	145.12441		<0.09
(3, 2) (2, 2) *E*	145.12620		0.290±0.030[b]
(3, −2) (2, −2) *E*	145.12635		
(3, 1) (2, 1) *E*	145.13188		0.263±0.030
(3, 2) (2, 2) *A*−	145.13346		0.106±0.026
(3, 0) (2, 0) *E*	145.09375	Jan. 7	0.059±0.015
(3, −1) (2, −1) *E*	145.09747		0.077±0.015
(3, 0) (2, 0) *A*+	145.10323		0.130±0.015
(3, 2) (2, 2) *A*	145.12441		0.052±0.014
(3, 2) (2, 2) *E*	145.12620		0.087±0.014[b]
(3, −2) (2, −2) *E*	145.12635		
(3, 1) (2, 1) *E*	145.13188		0.042±0.014
(3, 2) (2, 2) *A*−	145.13346		<0.045
(1, 1) (1, 0) *E*	165.05019	Nov. 14	0.166±0.036
(2, 1) (2, 0) *E*	165.06114		0.080±0.020
(3, 1) (3, 0) *E*	165.09931		0.090±0.033
(4, 1) (4, 0) *E*	165.19053		0.140±0.031
(5, 1) (5, 0) *E*	165.36944		0.210±0.036
(1, 1) (1, 0) *E*	165.05019	Nov. 21	0.184±0.042
(2, 1) (2, 0) *E*	165.06114		0.209±0.042
(3, 1) (3, 0) *E*	165.09931		0.299±0.042
(4, 1) (4, 0) *E*	165.19053		0.275±0.043
(5, 1) (5, 0) *E*	165.36944		0.350±0.040

[a] The line integrated intensities are from the autocorrelator when possible, from the 1 MHz filter bank otherwise; upper limits are 3σ.

[b] Blended with the previous line; the listed intensity is that of the blend.

The spatial distribution of the molecules was assumed to have a spherical symmetry around the nucleus (see below for a discussion of the anisotropy of the coma). All molecules were supposed to originate from the nucleus with a constant expansion velocity of 0.8 km s^{-1}, except H_2CO for which we also investigate below the possibility of a distributed origin over the coma. The lifetimes of the molecules are essentially limited by photodissociation in the solar UV field. We used the same photodissociation rates as in our previous studies (see also Crovisier (1994)), scaled with r_h^{-2}: 1.85×10^{-5} s^{-1} (HCN), 2.5×10^{-4} s^{-1} (H_2S), 2.0×10^{-4} s^{-1} (H_2CO) and 1.3×10^{-5} s^{-1} (CH_3OH).

The day-by-day values of the column density $<N>$ are summarized in Table 6 together with the production rates Q. Only the last two periods are considered here, as the larger beam offset from the nucleus makes a more detailed spatial modelling compulsory for Nov. 11–14 observations. Using for each period the H_2O production rates deduced from the OH observations at Nançay (Bockelée-Morvan *et al.*, 1994a), we deduce the relative production rates $Q/Q(H_2O)$. In January, the population inversion i of the OH maser was close to zero, and the signal-to-noise ratio on the line consequently poorer; furthermore, in this zone, the inversion curves computed by Despois *et al.* (1981) and Schleicher and A'Hearn (1988) are somewhat different, predicting i values of −0.15 and −0.22, respectively. Relative production rates based on the latter i value are given in brackets in Table 6.

4. Discussion

4.1. *Pre- and post-perihelion production rates*

From Table 6 it appears that the production rates relative to H_2O of the various molecules dropped by a factor of about 2 between November and January (i.e. between pre- and post-perihelion observations), whereas the heliocentric distance r_h and the H_2O production rate remained roughly constant. Further analysis will take into account the different jet/beam geometry between November and January and use a refined excitation model. As mentioned previously, higher collision rates seem to bring closer the relative abundances derived for the pre- and post-perihelion observations. Will all the differences between the November 21 and January observations be accounted for by geometry and excitation effects? This is a crucial question: if variations of the relative production rates of parent molecules are firmly established, this would constrain the scale of homogeneity of cometary matter under the hypothesis of a close match between the compositions of the nucleus and of the evaporated gases. Alternatively, such variations could be the consequence of differential outgassing from an originally homogeneous nucleus (cf. Espinasse *et al.*, 1991).

4.2. *Comparison with other comets*

A detailed comparison of the whole set of comets observed so far at millimetre wavelengths is in progress (Biver *et al.*, in preparation). We may note here that the relative abundances with respect to water of the various other parent molecules derived from the November 21 observations of P/Swift Tuttle are rather high when compared to other comets. The intensity of the molecular lines observed in November was indeed a surprise, when compared to the predictions based on either OH or total magnitude observations.

When compared to other comets (P/Halley, P/Brorsen Metcalf 1989 X, Austin 1990 V and Levy 1990 XX), abundances of HCN in P/Swift Tuttle on November 21 are higher by a factor of 2; those of H_2S and CH_3OH are 1.5 and 1.4 8 times those measured in Austin and Levy, respectively. Further studies and data on a larger sample of comets are needed in order to investigate whether these differences are due to modelling shortcomings, are cosmogonic or related to sublimation processes.

4.3. HCN *hyperfine ratio*

The expected intensities of the three HCN (1–0) hyperfine lines for LTE conditions are in the proportion 5:3:1. We measure $F(2\text{–}1)/F(1\text{–}1)$ ratios of 1.94 ± 0.22, 1.97 ± 0.20, 1.49 ± 0.40, respectively, for the mid-November, Nov. 21 and January observations. These values are within 2σ of the expected ratio 1.66. Note that fluorescence, like collisions, tends to enforce LTE ratios (see Appendix II in Despois *et al.* (1981)).

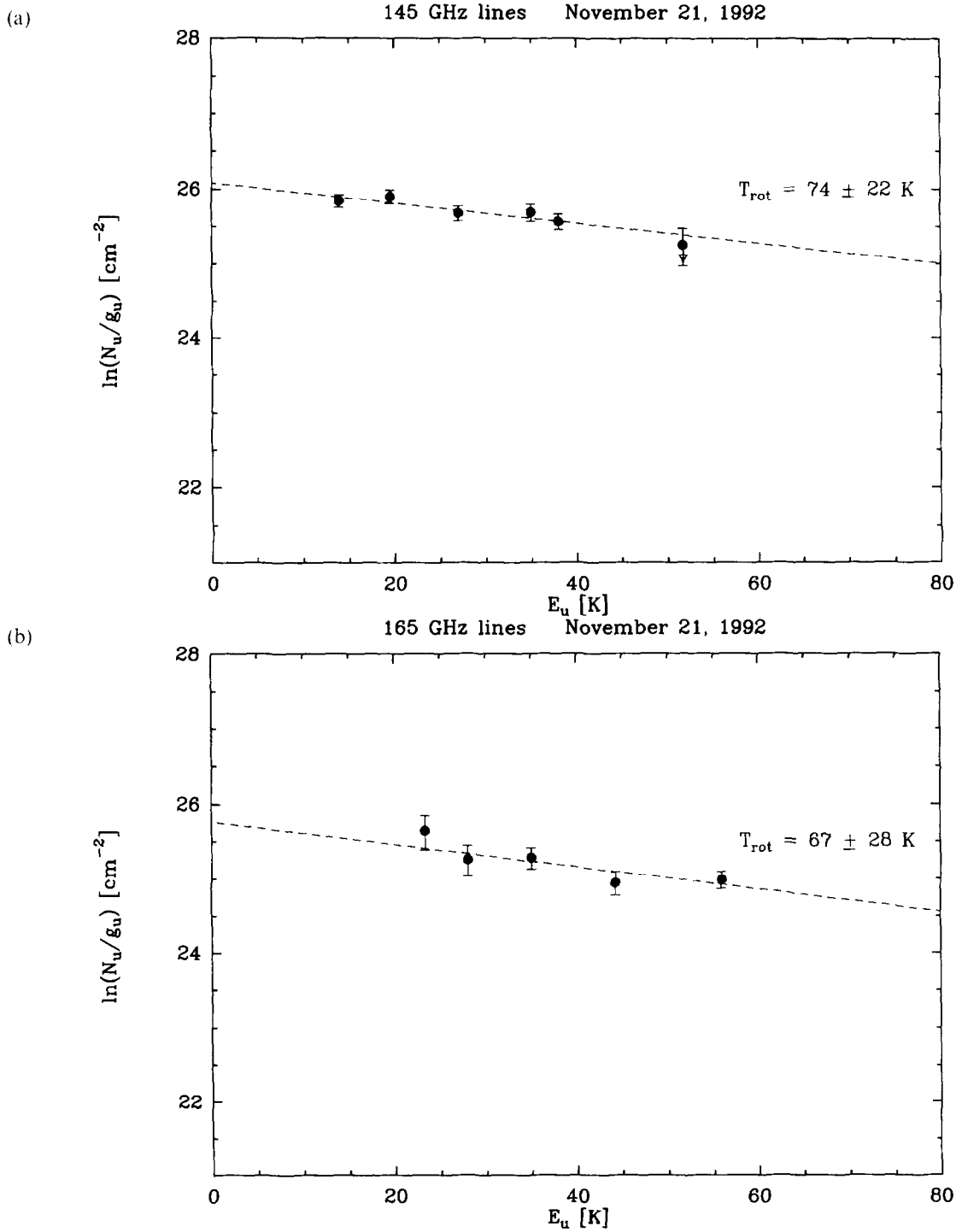

Fig. 3. Rotation diagrams for methanol lines observed in 109P/Swift–Tuttle at IRAM. These diagrams display the logarithm of the column density per sublevel N_u/g_u as a function of the energy of the upper level E_u, so that straight lines are expected for thermal equilibrium. Triangles refer to undetected lines and correspond to 3σ upper limits. Note that the plots for the 145 GHz (a) and 165 GHz (b) line groups on Nov. 21 have one level in common, (3,1) E at 34.98 K. On Jan. 1993 (c), the fit is poorer, suggesting deviations of the populations from thermal equilibrium

(c)

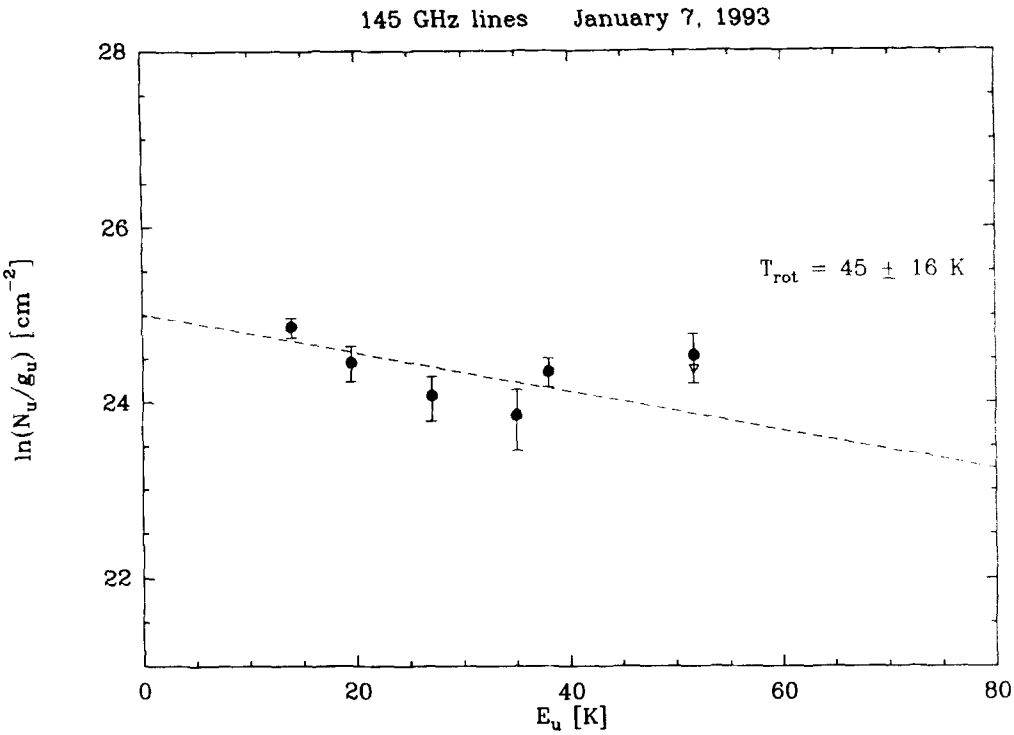

Fig. 3. (*Continued*).

4.4. H_2CO *source*

There are some indications that the H_2CO molecules (or at least part of them) come from an extended source (Schloerb and Ge, 1992; Meier *et al.*, 1993). By modelling this through a classical Haser distribution for daughter species with a scalelength of $L \sim 10{,}000$ km (cf. Colom *et al.*, 1992) the computed value for $Q(H_2CO)$ on Nov. 21 is increased from 2.1 to 4.1×10^{27} s^{-1}.

4.5. *Line shapes and velocity offsets*

It is the first time that cometary radio spectra show such a strong and unambiguous asymmetry and such large

Table 6. Molecular column densities averaged over the beam and production rates[a]

Molecule	Date[b]	$<N>$ [10^{12} cm^{-2}]	Q [10^{27} s^{-1}]	$Q/Q[H_2O]$ [%][c]		Model[d]
HCN	Nov. 21	0.93 ± 0.05	0.39 ± 0.02	0.098 ± 0.005		(1)
	Jan. 6–7	0.24 ± 0.03	0.17 ± 0.02	0.049 ± 0.006	[0.072]	
H_2S	Nov. 21	2.63 ± 0.31	1.45 ± 0.17	0.36 ± 0.04		(2)
H_2CO	Nov. 21	6.25 ± 0.17	2.10 ± 0.06	0.53 ± 0.01		(3)
	Jan. 6	1.08 ± 0.22	0.76 ± 0.15	0.22 ± 0.04	[0.32]	
CH_3OH 145 GHz	Nov. 21	148.0 ± 16.0	28.0 ± 3.0	7.0 ± 0.8		(4)
165 GHz		91.0 ± 25.0	16.0 ± 4.0	4.0 ± 1.1		
145 GHz	Jan. 7	23.0 ± 5.0	7.2 ± 1.5	2.1 ± 0.4	[3.0]	
H_2O	Nov. 21		400.0			
	Jan. 6–7		345.0 [237.]			

[a] A parent-molecule isotropic distribution is assumed. The effect of anisotropy, and of an extended source for H_2CO are discussed in the text. A mean coma temperature of 80 K in November and 40 K in January has been used. Collisional cross-sections are assumed to be 10^{-14} cm^2.

[b] No values are given for Nov. 11–14: due to the large offset from the nucleus, these measurements are especially sensitive to the anisotropy of the coma. For Nov. 21, the conversion of the column densities into production rates does not take into account the slight ephemeris offset.

[c] The $Q(H_2O)$ data are from Nançay observations (Bockelée-Morvan *et al.*, 1994a). Within square brackets, values derived using the Schleicher and A'Hearn (1988) inversion curve for the determination of $Q(H_2O)$.

[d] References for the excitation model: (1) Crovisier (1987); (2) Crovisier *et al.* (1991); (3) Bockelée-Morvan and Crovisier (1992); (4) column densities and production rates result from the rotation diagram analysis following Bockelée-Morvan *et al.* (1994b); the error bars do not include uncertainties in the derived rotational temperatures.

velocity offsets (see Figs 1 and 2 and Table 4). In our present data, all lines of all molecules which were observed with a sufficient signal-to-noise ratio exhibit the same behaviour, a strong peak at negative velocity (with respect to the computed nucleus velocity). This is also confirmed by OH observations at Nançay (Bockelée-Morvan *et al.*, 1994a; Colom *et al.*, 1993) and by millimetre line observations at JCMT (Bockelée-Morvan *et al.*, 1994c) and CSO (Schloerb *et al.*, 1993). This is thus undoubtedly linked to the global shape and motion of the coma of P/Swift–Tuttle, in which optical observations have shown a pronounced jet structure (e.g. Jorda *et al.*, 1994).

The general agreement between the line shapes of H_2CO and HCN is remarkable, as these species have different lifetimes (5.0×10^3 and 5.4×10^4 s, respectively, at 1 AU), have been observed with different beams (27″ and 12″) and may have a different origin (nuclear or extended source). Some indications on the latter problem might be gained when a detailed modelling of the coma and of the resulting line shapes has been completed.

4.6. *Anisotropy*

How does the anisotropy of the coma affect the derived production rates? As long as the telescope beam aims at the nucleus, and the lifetime of the molecule is short, the effect is limited—there is only some enhancement of the collisions due to a higher density for a given radius, as the molecules are emitted in a smaller solid angle. If, however, the lifetime of the molecule is large enough, a large fraction of the molecules are outside the beam when they belong to a jet perpendicular to the line of sight, whereas molecules remain in the beam if the jet is along the line of sight.

Quantitative evaluations of this effect are in progress; preliminary results show that for such a jet, there is almost no correction for the short-lived species H_2S and H_2CO (a parent distribution being assumed for the latter), whereas the HCN and CH_3OH production rates vary by a significant factor with respect to the isotropic case. To be consistent, the H_2O production rate from the OH data should also be derived for a jet; we find however that the correction is rather small.

Note that we are probably not seeing a unique, narrow jet, as the line profile exhibits emission both at negative and positive velocities. This velocity dispersion may result from the presence of multiple jets, from a more isotropic source of molecules coexisting with the jet, or from the hydrodynamical structure of the jet itself (the molecules which are initially emitted in a narrow jet in the region close to the nucleus spreading out in all directions at larger distances). In any case the corrections to the derived production rates due to the spatial distribution of the molecules will be smaller than for a pure monodirectional jet.

5. Conclusions

We have observed comet P/Swift–Tuttle both before and after perihelion, and detected the four molecules we have searched for: HCN, H_2CO, H_2S, CH_3OH. The signal-to-noise ratio on some of the spectra is very good (up to 30) and will allow a detailed line profile analysis in a future work. The most noticeable feature of the lines is a pronounced cusp at negative velocities, where the line intensity reaches up to twice its peak value for positive velocities; this results in a blueshift of the computed mean velocity by an amount of $\sim -0.45\,\mathrm{km\,s^{-1}}$. This asymmetric line profile is most probably linked to the well-observed jet-like features in the optical images of the coma.

We derive column densities for these molecules using our previously developed excitation models. Applying the rotation diagram technique to the methanol lines, we derive an average rotational temperature of the coma of about 70 K in November, with possibly a lower value of 45 K in January.

We deduce absolute and relative production rates in the frame of an isotropic coma as a first step, and discuss the correction we expect due to anisotropy. Using an H_2O production rate $Q(H_2O)$ of 4.0×10^{29} molec. s^{-1} (Bockelée-Morvan *et al.*, 1994a), we deduce the following relative abundances in the coma for Nov. 21: $X(HCN) \sim 0.1\%$, $X(H_2S) \sim 0.4\%$, $X(H_2CO) \sim 0.5\%$, $X(CH_3OH) \sim 4$–7%. In the post-perihelion observations on Jan. 6–7, 1993, using $Q(H_2O) \sim 3.5 \times 10^{29}$ molec. s^{-1}, we get: $X(HCN) \sim 0.05\%$, $X(H_2CO) \sim 0.2\%$, $X(CH_3OH) \sim 2\%$. A nuclear source has been assumed for H_2CO, but the effect of using a distributed source was discussed in Section 5.

There is thus a decline by about a factor of 2–3 in the molecules other than water between these two periods. This needs to be further analysed with a non-isotropic model of the coma and a refined excitation model. If confirmed, this variation in the relative abundances of parent molecules has important consequences in terms of inhomogeneity of the cometary molecule sources, or alternatively in terms of differentiated sublimation.

Acknowledgements. We thank B. Marsden and the IAU Central Bureau for Astronomical Telegrams for providing us constantly with their best cometary elements. We are grateful to the IRAM Granada staff for efficient telescope operation, to M. Guélin and J. Cernicharo for kindly accepting on very short notice the changes in the observation schedule necessary for these observations. We thank the referees for their detailed review of the paper. This work was partly supported by the Programme national de planétologie of the Institut des sciences de l'univers and the Centre national de la recherche scientifique (URA 1757).

References

Bockelée-Morvan, D. and Crovisier, J., Formaldehyde in comets: II Excitation of the rotational lines. *Astron. Astrophys.* **264,** 282–291, 1992.

Bockelée-Morvan, D., Crovisier, J., Despois, D., Forveille, T., Gérard, E., Schraml, J. and Thum, C., Molecular observations of comets P/Giacobini–Zinner 1984e and P/Halley 1982i at millimetre wavelength. *Astron. Astrophys.* **180,** 253–262, 1987.

Bockelée-Morvan, D., Bourgois, G., Colom, P., Crovisier, J., Gérard, E. and Jorda, L., Observations of OH in P/Swift-Tuttle and in several recent weak comets with the Nançay radio telescope. *Planet. Space Sci.* **42,** 193–198, 1994a.

Bockelée-Morvan, D., Crovisier, J., Colom, P. and Despois, D., The rotational lines of methanol in comets Austin 1990 V and Levy 1990 XX. *Astron. Astrophys.* **287,** 647–665, 1994b.

Bockelée-Morvan, D., Padman, R., Davies, J. K. and Crovisier, J., Observations of submillimetre lines of CH_3OH, HCN and H_2CO in comet P/Swift–Tuttle with the James Clerk Maxwell Telescope. *Planet. Space Sci.* **42,** 655–662, 1994c.

Colom, P., Crovisier, J., Bockelée-Morvan, D., Despois, D. and Paubert, G., Formaldehyde in comets: I. Microwave observations of P Brorsen–Metcalf (1989X), Austin (1990 V) and Levy (1990 XX). *Astron. Astrophys.* **264,** 270–281, 1992.

Colom, P., Bockelée-Morvan, D., Bourgois, G., Crovisier, J., Gérard, E., Jorda, L., Despois, D. and Paubert, G., Radio observations of anisotropic outgassing in comets, in *Asteroids, Comets, Meteors* 1993, Lunar and Planetary Institute Contr. No. 810, p. 72. Houston, 1993.

Crovisier, J., Rotational and vibrational synthetic spectra of linear parent molecules in comets. *Astron. Astrophys. Suppl.* **68,** 223–258, 1987.

Crovisier, J., Infrared spectrum of comets, in *Infrared Astronomy with ISO* (edited by T. Encrenaz and M. F. Kessler), pp. 221–248. Nova Science, 1992a.

Crovisier, J., Radio spectroscopy of comets: recent results and future prospects, in *Asteroids Comets Meteors* 1991 (edited by A. W. Harris and E. Bowell), pp. 137–140. Lunar and Planetary Institute, Houston, 1992b.

Crovisier, J., Photodestruction rates for cometary parent molecules. *J. Geophys. Res. Planets* **99,** 3777–3781, 1994.

Crovisier, J., Despois, D., Bockelée-Morvan, D., Colom, P. and Paubert, G., Microwave observations of hydrogen sulfide and searches for other sulfur compounds in comets Austin (1989c1) and Levy (1990c). *Icarus* **93,** 246–258, 1991.

Despois, D., Gérard, E., Crovisier, J. and Kazès, I., The OH radical in comets: observation and analysis of the hyperfine microwave transitions at 1667 MHz and 1665 MHz. *Astron. Astrophys.* **99,** 320–340, 1981.

Espinasse, S., Klinger, J., Ritz, C. and Schmitt, B., Modeling of the thermal behavior and of the chemical differentiation of cometary nuclei. *Icarus* **92,** 350–365, 1991.

Guilloteau, S., Spectral line calibration of the 30-m and 15-m antennas. IRAM Tech. Report, 1987.

Jorda, L., Colas, F. and Lecacheux, J., The dust jets of comet P/Swift–Tuttle 1992 XXVIII. *Planet. Space Sci.* **42,** 699–704, 1994.

Kiuchi, T., Periodic comet Swift–Tuttle (1737 II = 1862 III = 1992 t). IAU Circ. No. 5620, 1992.

Marsden, B. G., The next return of the comet of the Perseid meteors. *Astron. J.* **78,** 654–662, 1973.

Marsden, B. G., Williams, G. V., Kronk, G. W. and Waddington, W. G., Update on comet Swift–Tuttle. *Icarus* **105,** 420–426, 1993.

Mauersberger, R., Guélin, M., Martin-Pintado, J., Thum, C., Cernicharo, J., Hein, H. and Navarro, S., Line calibrators at λ = 1.3, 2 and 3 mm. *Astron. Astrophys. Suppl.* **79,** 217–261, 1989.

Meier, R., Eberhardt, P., Krankowsky, D. and Hodges, R. R., The extended formaldehyde source in comet P Halley. *Astron. Astrophys.* **277,** 677–690, 1993.

Schiaparelli, J. V., Sur la relation qui existe entre les comètes et les étoiles filantes. *Astron. Nachr.* **68,** 331–332, 1867.

Schleicher, D. G. and A'Hearn, M. F., The fluorescence of cometary OH. *Astrophys. J.* **331,** 1058–1077, 1988.

Schloerb, F. P. and Ge, W., Submillimeter molecular line observations of comet Levy (1990c), in *Asteroids Comets Meteors* 1991 (edited by A. W. Harris and E. Bowell), pp. 533–536. Lunar and Planetary Institute, Houston, 1992.

Schloerb, F. P., Kinzel, W. M., Swade, D. A. and Irvine, W. M., Observations of HCN in comet P Halley. *Astron. Astrophys. J.* **187,** 475–480, 1987.

Schloerb, F. P., Lis, D., Schilke, P., Sanders, D., Deane, J. and Ziurys, L., Observations of parent molecules in comet Swift–Tuttle. *Bull. Am. Astron. Soc.* **24,** 1000, 1993.

Sekanina, Z., Distribution and activity of discrete emission areas on the nucleus of periodic comet Swift–Tuttle. *Astron. J.* **86,** 1741–1773, 1984.

Womack, M. and McKeown, S. M., Millimeter-wavelength spectra of H_2CO and CH_3OH in comet Swift–Tuttle. *Bull. Am. Astron. Soc.* **24,** 999, 1993.

Wootten, A., Latter, W. B. and Despois, D., HCN emission from comet P Swift–Tuttle 1992t. *Planet. Space Sci.* **42,** 727–732, 1994.

Yau, K., Yeomans, D. K. and Weissman, P., The past and future motion of comet P Swift–Tuttle. *Mon. Not. R. Astron. Soc.* **266,** 305–316, 1993.